

Concept Unlearning by Modeling Key Steps of Diffusion Process

Chaoshuo Zhang
Xi'an Jiaotong University

ChaoshuoZhang@stu.xjtu.edu.cn

Le Yang
Xi'an Jiaotong University
yangle15@xjtu.edu.cn

Chenhao Lin
Xi'an Jiaotong University
linchenhao@xjtu.edu.cn

Qian Wang
Wuhan University
qianwang@whu.edu.cn

Zhengyu Zhao
Xi'an Jiaotong University
zhengyu.zhao@xjtu.edu.cn

Chao Shen
Xi'an Jiaotong University
chaoshen@mail.xjtu.edu.cn

Abstract

Text-to-image diffusion models (T2I DMs), represented by Stable Diffusion, which generate highly realistic images based on textual input, have been widely used. However, their misuse poses serious security risks. While existing concept unlearning methods aim to mitigate these risks, they struggle to balance unlearning effectiveness with generative retainability. To overcome this limitation, we innovatively propose the Key Step Concept Unlearning (KSCU) method, which ingeniously capitalizes on the unique step-wise sampling characteristic inherent in diffusion models during the image generation process. Unlike conventional approaches that treat all denoising steps equally, KSCU strategically focuses on pivotal steps with the most influence over the final outcome by dividing key steps for different concept unlearning tasks and fine-tuning the model only at those steps. This targeted approach reduces the number of parameter updates needed for effective unlearning, while maximizing the retention of the model's generative capabilities. Through extensive benchmark experiments, we demonstrate that KSCU effectively prevents T2I DMs from generating undesirable images while better retaining the model's generative capabilities. Our code will be released.

1. Introduction

In recent years, the advancement of text-to-image (T2I) diffusion models [9, 16, 20, 22, 26, 43] has led to their widespread adoption across various domains [1, 27, 31, 38, 42], including short videos, comics, and illustrations. As a result, AI-generated images have become an integral part of daily life for many individuals. However, large-scale T2I models are trained on extensive datasets [4, 37, 38, 45] that

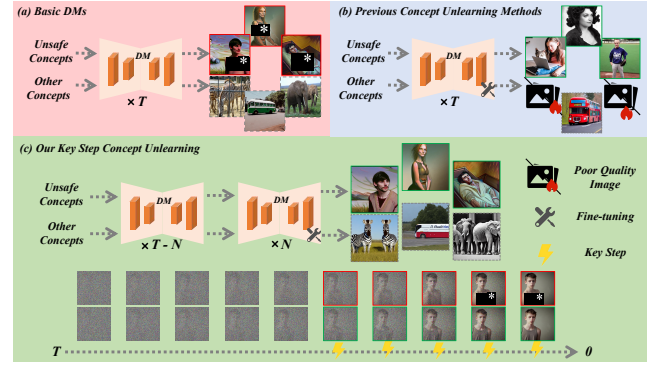


Figure 1. Compared to previous methods (b), KSCU (c) focuses exclusively on the denoising steps that have the most significant impact on concept generation and achieves effective forgetting of the target concept while better preserving the generation of unrelated concepts.

often contain sensitive content, such as unauthorized artistic works [46, 47] or Not Safe For Work (NSFW) material. Consequently, these models can inadvertently regenerate infringing content when prompted with relevant text inputs [3]. This raises significant concerns regarding copyright infringement and social security risks, highlighting the urgent need for effective mitigation strategies.

The generation of NSFW content poses a major security risk for mainstream text-to-image diffusion models. Researchers have explored various approaches to mitigate this issue, including dataset-based screening, content filtering [39], and fine-tuning techniques [7, 30, 41]. Concept unlearning, as a fine-tuning-based approach [11, 13, 14, 18, 23, 53, 56], selectively adjusts partial model parameters to remove the model's ability to generate specific concepts. Through concept unlearning, T2I diffusion models effectively 'forget' designated visual concepts by replacing them with semantically neutral content. This targeted parameter adjustment (referred to as "concept erase" [12, 14, 21])

provides distinct advantages over conventional methods—offering greater robustness than post-hoc filtering [39] while avoiding the intensive labor of dataset curation [40], and has become one of the most promising approaches to curb the generation of NSFW content in T2I propagation models.

Although significant progress has been made in concept unlearning for T2I diffusion models, several challenges remain unresolved. **a. Blind unlearning of the entire diffusion process.** Existing concept unlearning approaches for T2I diffusion models fail to notice for the stepwise denoising characteristics of diffusion models. Since diffusion models generate images through a progressive denoising process—where earlier steps primarily capture low-frequency structural information and later steps refine high-frequency details [2, 17, 35, 50, 55]—unlearning does not necessarily require fine-tuning across all denoising steps. **b. Unbalanced unlearning effectiveness and generative retainability.** Most existing methods require extensive modifications to the original model parameters to ensure unlearning effectiveness. However, excessive parameter updates may lead to over-unlearning, negatively affecting the model’s ability to generate unrelated concepts. Conversely, strictly limiting the scale of parameter updates to preserve generative retainability—i.e., the model’s ability to retain generation quality for unrelated concepts—makes it difficult to fully unlearn the target concept. **c. Robustness at high cost.** Adversarial attack [6, 51, 58] research on unlearned models has demonstrated that carefully crafted adversarial text prompts can successfully recover unlearned concepts. While adversarial training [21, 59] can enhance robustness against such attacks, it is computationally expensive and brings low generative retainability.

To address existing challenges, we propose Key Step Concept Unlearning (KSCU), a novel framework for concept unlearning in T2I diffusion models. Unlike prior methods that operate across all denoising steps, KSCU selectively fine-tunes a subset of key steps based on a predefined Key Step Table. For different unlearning tasks, multiple step intervals are empirically defined, and a selection algorithm prioritizes steps with the greatest influence on the final output, enabling efficient and targeted unlearning. To improve robustness, KSCU applies Prompt Augmentation in the final training stage, including random shuffling, word removal, character insertion, and embedding noise. These augmented prompts help the model better capture the semantic distribution of the unlearned concept in the embedding space. Additionally, we introduce a Key Step Unlearning Loss tailored to classifier-free guidance DMs. By combining Key Step Table, Prompt Augmentation, and Key Step Unlearning Loss, KSCU achieves more effective concept unlearning while better ensuring generative retainability.

Our contributions can be summarized as follows:

- We propose KSCU, a novel concept unlearning framework for T2I DMs. Unlike prior work, KSCU only performs fine-tuning for the key step, achieving efficient unlearning by applying smaller adjustments to the model, thereby maintaining the model’s generation ability, taking both unlearning effectiveness and generative retainability into account.
- Our proposed KSCU integrates three innovations: Key Step Table, a step selection strategy focusing on critical denoising steps to achieve effective concept unlearning with minimal fine-tuning overhead; Prompt Augmentation to enhance robustness by introducing diverse prompt variations; and Key Step Unlearning Loss, a concept unlearning loss tailored for classifier-free guided diffusion models, enabling effective concept removal while preserving generation quality.
- Extensive experimental results on multiple datasets demonstrate the superiority of KSCU. For instance, in the NSFW unlearning experiment, KSCU achieves a remarkable unlearning accuracy of 96.5% with FID of just 14.1, significantly outperforming the previous SOTAs.

2. Related Work

2.1. Text-to-Image Diffusion Models

Diffusion models [17] were initially proposed as a generative framework based on the reverse denoising process to reconstruct target input images. With the introduction of advanced techniques such as score-based models [50], noise-conditioned score network [49], and denoising-based guidance [9], these models have become increasingly popular for text-to-image (T2I) generation. The emergence of latent diffusion models (LDMs) [40] and classifier-free guidance [16] has further improved the controllability and efficiency of diffusion-based T2I systems. Their ability to generate high-quality, semantically coherent images has established diffusion models as the dominant approach in T2I generation.

Building on these advancements, recent research has focused on optimizing T2I diffusion models in terms of efficiency, scalability, and applicability. Significant breakthroughs have been made in acceleration algorithms [25, 28, 29, 48], model architectures [40], and large-scale datasets [4, 37, 38, 45], all of which have contributed to the widespread adoption of these models in practical applications [1, 31, 38, 42]. However, despite their advantages, these models are vulnerable to misuse, leading to concerns over NSFW content [39], unauthorized depictions of individuals, and copyright-infringing artwork [1]. As T2I diffusion models continue to advance in realism and fidelity, addressing their ethical and legal challenges has become an urgent priority for the research community.

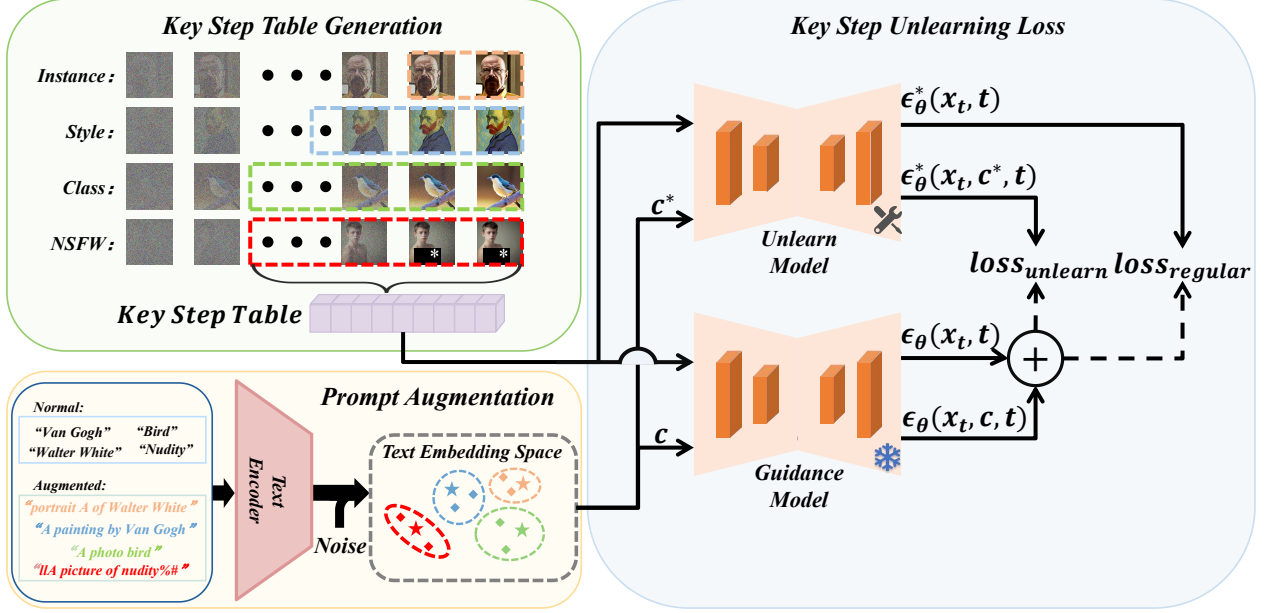


Figure 2. The KSCU framework consists of three key modules: Key Step Unlearning Loss, Key Step Table, and Prompt Augmentation. The Key Step Table predefines step selection strategies for four concept unlearning tasks (Class, Style, NSFW, and Instance). During training, a denoising step t is selected from the Key Step Table. The unlearn model performs denoising sampling to obtain x_t , while the Prompt Augmentation module converts the target concept c into an augmented prompt c^* . Using x_t , t , c , and c^* , the Key Step Unlearning Loss is computed via Equation (7), and designated parameters of the unlearn model are updated through backpropagation.

2.2. Diffusion Model Concept Unlearning

Large-scale datasets [4, 37, 38, 45] often contain undesirable data, including content with inherent biases, ethically problematic information, or copyrighted materials that may later become restricted. Models trained on such datasets acquire the ability to generate this sensitive content, posing significant security and ethical risks in text-to-image (T2I) generation. To mitigate these concerns, concept unlearning in diffusion models has been proposed, aiming to selectively erase specific generative capabilities while preserving the model’s ability to generate unrelated content—without requiring full retraining.

Several existing methods have been developed for concept unlearning in T2I diffusion models. ESD [12] and CA [23] employ a frozen guiding model to provide negative guidance for fine-tuning. UCE [13] and RECE [14] leverages a closed-form solution to modify cross-attention weights, enabling simultaneous unlearning of multiple concepts. Salun [11] and Scissorhands [52] optimize parameter updates based on their influence on concept retention. Meanwhile, RACE [21] and AdvUnlearn [59] generate adversarial samples to enhance unlearning and improve model robustness.

Although concept unlearning methods provide a certain level of security for T2I diffusion models, their effectiveness remains questionable when faced with diverse real-

world scenarios and adversarial examples. Recent studies on adversarial attacks [6, 51, 58] against T2I DMs indicate that existing concept unlearning methods remain vulnerable to such attacks. To enhance robustness, current approaches rely on increasing the number of fine-tuning iterations or incorporating adversarial training [21, 59]. However, these methods significantly increase computational cost while further degrading the model’s generative quality.

Unlike previous approaches [12, 23, 33, 53], KSCU explicitly considers the relationship between the stepwise denoising process of diffusion models and the effectiveness of concept unlearning. Instead of modifying the model across all denoising steps, KSCU selectively applies unlearning to specific denoising steps that contribute most significantly to the target concept’s generation. This targeted approach reduces the number of training iterations required for unlearning, thereby minimizing unnecessary parameter adjustments and preserving the model’s overall generative quality.

3. Key Step Concept Unlearning

As shown in Figure 2, our framework consists of three main components: the Key Step Unlearning Loss module, including the unlearn model that undergoes fine-tuning and the guidance model that provides reverse guidance; the Key Step Table module, which controls the denoising steps during training; and the Prompt Augmentation module to help

the model learn more generalized semantic distribution of the unlearned concept in the text embedding space.

3.1. Background

Diffusion models [17] are a class of generative models that learn data distributions by gradually denoising a normally distributed variable. The process consists of two phases: the forward diffusion process and the reverse denoising process. In the forward process, Gaussian noise is incrementally added to the data over a series of time steps, transforming the data into a nearly isotropic Gaussian distribution. Conversely, the reverse process learns to iteratively denoise the data, recovering the original distribution.

Latent Diffusion Models. While traditional diffusion models operate directly in the high-dimensional data space, latent diffusion models (LDMs) [40] introduce a more efficient approach by performing the diffusion process in a compressed latent space. LDMs first employ an autoencoder to encode the input data \mathbf{x} into a lower-dimensional latent representation $\mathbf{z} = E(\mathbf{x})$, where E is the encoder. The diffusion process is then applied to \mathbf{z} instead of \mathbf{x} , significantly reducing computational complexity.

The key distinction of LDMs lies in their separation of the diffusion process from the high-dimensional data space. The forward process in the latent space is defined as:

$$q(\mathbf{z}_t | \mathbf{z}_{t-1}) = \mathcal{N}(\mathbf{z}_t; \sqrt{1 - \beta_t} \mathbf{z}_{t-1}, \beta_t \mathbf{I}), \quad (1)$$

where \mathbf{z}_t is the latent representation at time step t . The reverse process learns to denoise the latent representation:

$$p_\theta(\mathbf{z}_{t-1} | \mathbf{z}_t) = \mathcal{N}(\mathbf{z}_{t-1}; \mu_\theta(\mathbf{z}_t, t), \Sigma_\theta(\mathbf{z}_t, t)). \quad (2)$$

After the reverse process, the decoder D maps the denoised latent representation \mathbf{z}_0 back to the data space: $\mathbf{x} = D(\mathbf{z}_0)$. This two-stage approach not only reduces computational costs but also enables the generation of high-resolution samples by focusing on a compact latent space.

Classifier-Free Guidance. Classifier-Free Guidance [16] is a technique designed to improve the controllability of diffusion models without relying on an external classifier. Instead of conditioning the model on explicit labels, classifier-free guidance jointly trains a conditional and an unconditional diffusion model. Formally, let $\epsilon_\theta(\mathbf{x}_t, t, \mathbf{c})$ denote the conditional prediction and $\epsilon_\theta(\mathbf{x}_t, t)$ denote the unconditional prediction, where \mathbf{c} is the conditioning information (e.g., a class label or text embedding). The guided prediction is computed as:

$$\hat{\epsilon}_\theta(\mathbf{x}_t, t, \mathbf{c}) = \epsilon_\theta(\mathbf{x}_t, t) + w \cdot (\epsilon_\theta(\mathbf{x}_t, t, \mathbf{c}) - \epsilon_\theta(\mathbf{x}_t, t)) \quad (3)$$

where w is the guidance scale controlling the strength of conditioning. A higher w emphasizes the conditioning information, while $w = 0$ reduces the model to an unconditional generator.



Figure 3. Sampling with "nudity woman" prompt reveals emergence of nudity concepts in the final 10 denoising steps.

3.2. Key Step Unlearning Loss

According to formula (3), in a classifier-free guidance diffusion model, the linear extrapolation of $\epsilon_\theta(\mathbf{x}_t, t, \mathbf{c})$ and $\epsilon_\theta(\mathbf{x}_t, t)$ serves as the gradient of the implicit classifier $\nabla_{\mathbf{x}_t} \log p(y | \mathbf{x}_t)$. Our objective is not to generate images corresponding to the text prompt \mathbf{c} , but rather to shift the model's predicted noise $\hat{\epsilon}_\theta(\mathbf{x}_t, t, \mathbf{c})$ in the opposite direction of $\nabla_{\mathbf{x}_t} \log p(y | \mathbf{x}_t)$. Furthermore, we exclusively fine-tune the conditional noise $\hat{\epsilon}_\theta(\mathbf{x}_t, t, \mathbf{c})$ to ensure that the generation of unrelated concepts remains unaffected. The fine-tuning objective is formulated as:

$$\begin{aligned} \hat{\epsilon}_\theta^*(\mathbf{x}_t, t, \mathbf{c}) &= \epsilon_\theta(\mathbf{x}_t, t) - w \cdot (\epsilon_\theta(\mathbf{x}_t, t, \mathbf{c}) - \epsilon_\theta(\mathbf{x}_t, t)) \\ &= \epsilon_\theta(\mathbf{x}_t, t) + w \cdot (\hat{\epsilon}_\theta(\mathbf{x}_t, t, \mathbf{c}) - \epsilon_\theta(\mathbf{x}_t, t)) \end{aligned} \quad (4)$$

From this, we derive the unlearning loss:

$$\text{Loss}_{\text{unlearn}} = \|\hat{\epsilon}_\theta^*(\mathbf{x}_t, t, \mathbf{c}) - (\epsilon_\theta(\mathbf{x}_t, t) - (\epsilon_\theta(\mathbf{x}_t, t, \mathbf{c}) - \epsilon_\theta(\mathbf{x}_t, t)))\|_2 \quad (5)$$

where $\hat{\epsilon}_\theta^*$ represents the unlearned model, ϵ_θ is the guidance model, \mathbf{x}_t denotes the denoised image at step t , and \mathbf{c} corresponds to the text prompt.

More importantly, the Key Step Unlearning Loss also accounts for the optimization of unconditional noise. To preserve the model's ability to generate unrelated concepts, we introduce a regularization term based on unconditional noise prediction to minimize parameter changes. Specifically, we constrain the L2 distance between the unconditional noise predictions of the guidance and unlearned models, offering partial protection for shared parameters. Additionally, we observe that unconditional noise, which uses the previous sampling step as a prior, gradually aligns with the target concept as denoising progresses. As shown in Figure 3, we use the prompt "nudity woman" with DDIM steps set to 50 and sample images using Stable Diffusion v1-4. From left to right, the images correspond to step = 40, step = 50, and the last 10 steps sampled using only unconditional noise. The qualitative results show that even unconditional noise alone causes the generation to drift toward the "nudity" concept. This highlights the necessity of applying unlearning not only to the conditional branch but also

Algorithm 1 Key Step Table Generation

Input: start step S , end step E , table length L , full loops before shift $loop_n$

Output: $KeyStepTable[: L]$

```
1:  $KeyStepTable \leftarrow None$ 
2:  $s_{cur} \leftarrow S$ 
3:  $loop_{cur} \leftarrow 0$ 
4: while  $len(KeyStepTable) < L$  do
5:    $KeyStepTable \leftarrow KeyStepTable \cup [s_{cur}, s_{cur} + 1, \dots, E]$ 
6:    $loop_{cur} \leftarrow loop_{cur} + 1$ 
7:   if  $loop_{cur} = loop_n$  then
8:      $s_{cur} \leftarrow \min(s_{cur} + 1, E - 1)$ 
9:      $loop_{cur} \leftarrow 0$ 
10:  end if
11: end while
```

to the unconditional branch in classifier-free guidance diffusion models. Accordingly, we apply unlearning training to the unconditional component as well. The regularization loss is formulated as:

$$Loss_{regular} = \|\epsilon_{\theta}^*(\mathbf{x}_t, t) - ((1 + \lambda_1)\epsilon_{\theta}(\mathbf{x}_t, t) - \lambda_1 \epsilon_{\theta}(\mathbf{x}_t, t, \mathbf{c}))\|_2^2 \quad (6)$$

where λ_1 needs to be a small value that is linearly related to t . For t from 1000 to 0, we set $\lambda_1 = (1000 - t)/(2 * 10^5)$

The final Key Step Unlearning Loss function for KSCU is defined as:

$$Loss = Loss_{unlearn} + \lambda_2 \cdot Loss_{regular} \quad (7)$$

where $\lambda_2 = 1 \times 10^{-4}$ in KSCU.

3.3. Key Step Table Generation

The goal of concept unlearning is to prevent the generation of a target concept. Due to the nature of diffusion-based generation, high-frequency details in the image are primarily refined during the later denoising steps. Therefore, we hypothesize that these later steps play a more critical role in the unlearning process. To validate this, we design a preliminary experiment using ESD [12] to fine-tune Stable Diffusion v1-4, while restricting the range of training steps. The results show that, for NSFW content unlearning, training only the last 70% of denoising steps (with the total number of training iterations also reduced to 70% of the original) preserves approximately 95% of the unlearning accuracy observed when training across all steps. This indicates that, compared to early steps, the later steps contribute more significantly to concept forgetting. Limiting unlearning to these steps—those responsible for high-frequency detail generation—can still achieve effective unlearning performance.

Based on the above observation, we design a step selection algorithm to generate Key Step Table. The Key

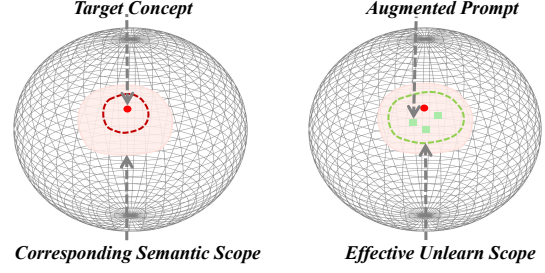


Figure 4. Comparison of Semantic Range in Prompt Embedding Space. Left: Limited effective unlearning semantic range (red dashed boundary) with single target concept prompts. Right: Expanded effective unlearning semantic range (green dashed boundary) using augmented prompts.

Step Table consists of incrementally growing step intervals and shifts the starting point forward after a fixed number of loops to progressively cover a broader range of late denoising steps. As shown in Algorithm 1, the algorithm constructs the Key Step Table from a given starting step S to an ending step E . In each iteration, the full interval from s_{cur} to E is appended to the Key Step Table. After $loop_n$ iterations, the starting step s_{cur} is shifted forward by one, and the process is repeated until the Key Step Table reaches the desired length L . This mechanism ensures that training focuses more on later denoising steps, which are more influential, while avoiding overfitting to a single segment.

Furthermore, our analysis indicates that the most influential steps vary by concept type. Specifically, for NSFW content and class unlearning, the last 70% of denoising steps are most critical, whereas for style unlearning, only the last 50% of steps play a dominant role, while for individual instance forgetting, this interval can be further reduced to the last 20%. These observations highlight the need for a structured step selection approach.

3.4. Prompt Augmentation

For prompt-based concept unlearning in T2I DMs, the objective is to erase undesired visual concepts from the model’s generated results. Prompts describe these visual concepts to explicitly specify the target concept for unlearning. However, accurately depicting a complex visual concept through textual prompts is often challenging. Inaccurate prompts may lead to incomplete unlearning, where related concepts remain, or incorrect removal of unrelated concepts. Recently, many methods [5, 54] have recognized this issue and introduced improvements targeting prompt section. In this section, we propose a simpler yet effective Prompt Augmentation method to address this problem.

For a given concept c to be unlearned, we use large language models such as ChatGPT [32] and DeepSeek [8] to generate ten augmentation rules that expand the original concept into diverse textual descriptions. For example,

given the concept "cat" and the rule "a picture of {}", we obtain: "a picture of a cat". We then introduce perturbations by randomly inserting scrambled characters, shuffling word order, or removing non-keywords. Additionally, Gaussian noise is injected into the text embeddings of these modified descriptions [19]. Since the embeddings are ultimately perturbed, the quality of the augmentation rules need not be strictly controlled.

As shown in Figure 4, in the embedding space [36], nearby vectors share similar semantics and induce similar generative behavior. Leveraging this property, Prompt Augmentation enables the model to better perceive the semantic space of the target concept during unlearning, leading to more effective concept erasure. Theoretically, Prompt Augmentation constructs numerous embeddings close to the target concept, aligning with its semantic distribution. This allows the model to unlearn not only the concept itself but also its semantic variations. In contrast, adversarial samples are discrete and harder to construct. Compared to adversarial training, which is costly in time and computation, Prompt Augmentation offers a more efficient alternative for enhancing unlearning robustness.

4. Experimental Results

4.1. Experimental Setup

Dataset. To rigorously evaluate various concept unlearning methods, we conducted experiments on four concept unlearning task types: Class, Style, NSFW, and Instance on two datasets, including the *I2P* [44] and *Unlearn Canvas* [57].

I2P is a dataset containing 4,703 NSFW prompts. For our experiments, we selected 931 prompts labeled as "sexual" to generate images. We then used *Nudenet* [34] (threshold = 0) to analyze the generated images, detecting 575 nudity regions in the outputs from these 931 prompts. Across the entire *I2P* dataset, *Nudenet* identified a total of 793 nudity regions. This dataset setting reduced the computational cost while still preserving the majority of the experimental requirements.

Unlearn Canvas is a recently released dataset comprising 20 classes and 60 distinct styles of high-resolution stylized images. Since testing the entire dataset was computationally intensive, we selected 10 classes and 10 styles for the evaluation, including the following:

- **Class:** Architectures, Bears, Cats, Dogs, Humans, Towers, Flowers, Sandwiches, Trees, Sea.
- **Styles:** Abstractionism, Artist Sketch, Cartoon, Impressionism, Monet, Pastel, Pencil Drawing, Picasso, Sketch, Van Gogh.

Such the selection also ensured diversity: the chosen classes include animals, plants, natural scenes, and man-made objects, while the styles cover both artistic styles such

as "Monet" and illustrative styles such as "Sketch".

Evaluation. In our experiments, we evaluated the unlearning effectiveness of various methods using Unlearn Accuracy (UA) originally from [12]. To achieve a more concise and effective evaluation of unlearning effectiveness, we computed UA as follows: $UA = 1 - x/y$. In the *I2P* dataset, x represented the number of nudity regions detected in the output images by the unlearned model, and y was 575. Compared to previous methods [12] that evaluated each exposed region individually, we aggregated all cases into a single metric, Unlearn Accuracy, which offered a more concise, analyzable and convincing measure of unlearning performance. For the *Unlearn Canvas* dataset, x denoted the number of target concepts detected by the classifier [10], while y corresponded to the total number of generated images based on the target prompts.

We also utilized the Fréchet Inception Distance (FID) [15], a widely used metric for assessing the quality of generated images, which measured the distance between the generated and real images in feature space. In the *I2P* dataset, we generated images from corresponding prompts using the *COCO* [24] dataset and computed the FID by comparing them with real images from coco30k to assess how well each baseline preserved the model's generative capacity. For *Unlearn Canvas*, we generated images using the prompt "A {class} image in {theme} style.", then calculated the FID by comparing these images with real images from the *Unlearn Canvas* dataset. Besides UA and FID, *Unlearn Canvas* introduced two additional metrics: In-domain Retain Accuracy (IRA) and Cross-domain Retain Accuracy (CRA), which helped evaluate the model's ability to retain relevant information. Lastly, we assessed the model's defense capabilities by constructing adversarial text prompts using the P4D [6] and UnlearnDiff(UDA) [58] methods based on *I2P* prompts, comparing them using Attack Success Rate (ASR).

Baseline and Training Details. To provide a comprehensive comparison of various methods, we selected six state-of-the-art (SOTA) unlearning techniques, including ESD [12], CA [23], FMN [56], EDiff [53], Salun [11], and SHS [52]. For KSCU's training setup, we used a batch size of 1. The scheduler was set to 50 timesteps. For style unlearning tasks, the Key Step Table was configured to start from step 25 and end at step 50. For other tasks, the training Key Step Table began at step 15. We employed the Adam optimizer with a learning rate of 1×10^{-5} , applying a total of 750 parameter updates. For all baseline methods, we adopted the default hyperparameters as specified in their original papers. We employed DDIM for denoising, using 50 steps. For *Unlearn Canvas*, we used Stable Diffusion 1.5, while for all other experiments, unless explicitly stated otherwise, Stable Diffusion 1.4 was used. All experiments were conducted on a single Nvidia L40 GPU.

Table 1. Class and Style Unlearning Performance on Unlearn Canvas. The bold font represents the best, and the underlined font represents the second-best.

Method	class				style			
	UA(%) \uparrow	IRA(%) \uparrow	CRA(%) \uparrow	FID \downarrow	UA(%) \uparrow	IRA(%) \uparrow	CRA(%) \uparrow	FID \downarrow
ESD [12]	68.6	98.9	96.4	26.1	100.0	85.7	99.0	25.3
CA [23]	32.5	86.7	83.4	51.9	96.0	86.6	88.7	37.4
FMN [56]	25.9	93.0	96.1	36.8	41.5	<u>95.1</u>	91.3	28.5
EDiff [53]	78.0	94.1	90.1	48.2	67.5	93.7	98.3	39.8
Salun [11]	51.3	93.5	94.6	47.9	17.5	96.3	95.2	34.8
SHS [52]	62.5	54.6	56.7	79.4	65.0	51.1	29.4	65.9
KSCU	<u>70.0</u>	99.0	97.1	25.8	100.0	88.7	99.3	23.1

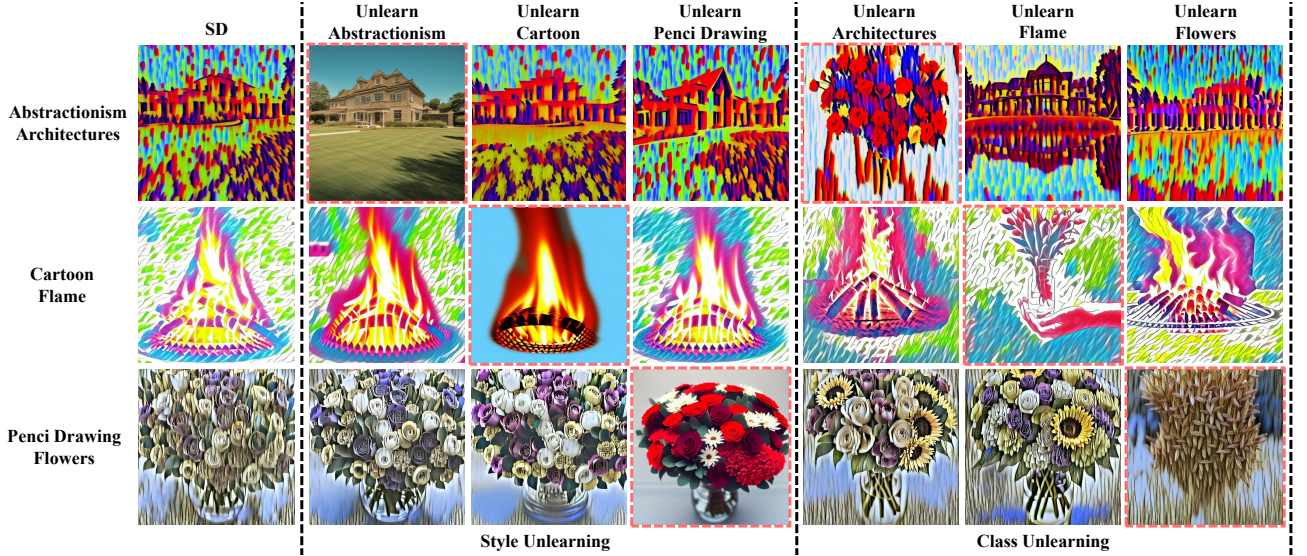


Figure 5. The figure demonstrates KSCU’s unlearning effectiveness and generative retainability on *Unlearn Canvas*. Images within the red border show the removal of target concepts, while images outside the red border highlight KSCU’s generative retainability. KSCU only aims to remove the target concept without enforcing constraints on the final output. In Appendix, we provide a controllable version of KSCU that can replace the target concept with any specified alternative concept.

4.2. Class and Style Unlearning

To evaluate the effectiveness of our proposed KSCU, we first performed qualitative experiments on class and style unlearning tasks. As shown in Figure 5, for different image samples, KSCU has completely blocked the generation of the target class or style, with minimal impact on unrelated classes and styles. Then we quantitatively evaluated its performance, as described below.

Class Unlearning. In the selection of test categories for class unlearning, we randomly selected ten classes encompassing a diverse range from *Unlearn Canvas*, including animals, plants, man-made objects, and natural elements. The experimental results presented in Table 1 indicated that KSCU achieved superior category-wide unlearning while better preserving the model’s generative capability—an advantage not observed in other SOTAs.

Specifically, as illustrated in Table 1, KSCU achieved 70%, 99.0%, 97.1%, and 25.8 on UA, IRA, CRA, and FID, respectively. In terms of UA, KSCU ranked as the second-best method, while it achieved the best performance on IRA, CRA, and FID. A method that aggressively removed target concepts might achieve higher UA but often at the cost of severely compromising image quality and diversity. Conversely, an overly conservative method may ensure generative retainability but fail to achieve effective unlearning. Therefore, evaluating a T2I diffusion model unlearning method requires consideration of both unlearning effectiveness (UA) and generative retainability (IRA, CRA, FID). In these two regards, KSCU demonstrates a more favorable trade-off. A high UA of 70% indicates strong unlearning effectiveness, while the best IRA and CRA scores confirm its superior ability to preserve generative diversity. Furthermore, KSCU outperforms all other SOTAs in FID,

indicating that its unlearned model can generate higher-quality images, further validating its generative retainability. Conversely, while EDiff attained the highest UA, its FID reached 48, suggesting that although it exhibited strong unlearning performance, it significantly degraded the model’s generative ability. This low generative retainability of EDiff indicates that it is difficult to use in practical applications.

Style Unlearning. We conducted experiments on image style unlearning using the *Unlearn Canvas* dataset. We quantitatively assessed the feasibility of removing artistic styles to address copyright concerns using the IRA and CRA metrics. Given computational constraints, we selected 10 styles from Section 4.1, covering three artistic styles and seven artistic representations. This selection ensured a diverse evaluation of style unlearning across different visual attributes while maintaining a feasible training cost. The experimental results presented in Table 1 indicated that KSCU achieved strong unlearning effectiveness and retainability, while maintaining a favorable balance between the two on the style unlearning task.

Specifically, as shown in Table 1, KSCU achieved scores of 100%, 88.7%, 99.3%, and 23.1 in UA, IRA, CRA, and FID, respectively. Among these, UA, CRA, and FID were the best across all compared methods. While KSCU’s IRA was slightly lower than the Salun method with very low unlearning effectiveness (UA = 17.5%), this method reached high IRA at the expense of insufficient concept forgetting. In contrast, when compared with other high unlearning effectiveness methods such as CA and ESD (UA > 95%), KSCU demonstrated clearly superior IRA, CRA, and FID. These results indicated that KSCU not only effectively eliminated traces of artistic styles but also better preserved the model’s ability to generate unrelated concepts.

KSCU halved the iteration count compared to ESD by selectively fine-tuning only the latter 50% of denoising steps. Despite reducing the number of parameter updates by half, KSCU still outperformed ESD in style unlearning, reinforcing that full-step fine-tuning is unnecessary for concept unlearning in T2I diffusion models. Focusing on the most influential steps enables more efficient and controlled unlearning while minimizing disruptions to the model’s generative capacity. These findings suggest that the Key Step Table optimization strategy adopted by KSCU offers a more practical and scalable solution for concept unlearning in large-scale diffusion models.

4.3. NSFW Unlearning

NSFW Unlearning. In the NSFW concept forgetting experiment, we fine-tuned the models using “nudity” as the target concept and obtained the corresponding unlearned models. Each method used its corresponding unlearned model to generate 931 and 30,000 images based on prompts from the *i2p* [44] and *COCO* [24] datasets, respectively. Ta-

Table 2. Evaluation of Unlearning Capability on “Nudity”. The bold font represents the best, and the underlined font represents the second-best.

Method	UA(%) \uparrow	P4D(%) \downarrow	UDA(%) \downarrow	FID-30k \downarrow
ESD [12]	88.2	39.3	73.7	15.4
CA [23]	34.3	-	-	<u>15.3</u>
Salun [11]	100.0	0.0	4.2	67.9
FMN [56]	38.6	-	-	20.9
EDiff [53]	93.9	29.6	52.5	19.8
SHS [52]	84.3	62.2	95.5	18.1
KSCU	<u>96.5</u>	<u>23.2</u>	<u>47.2</u>	14.1

ble 2 presents the results, assessing the unlearning effectiveness of various methods using Unlearn Accuracy, P4D, and UDA’s ASR. FID is also compared to evaluate generative retainability. Note that CA and FMN, which fine-tune only the cross-attention module, show limited NSFW unlearning effects and are not further tested for robustness against attacks.

As shown in Table 2, KSCU balanced unlearning effectiveness and generative retainability, achieving a UA of 96.5%, surpassing other methods in forgetting capability. Meanwhile, its FID-30K of 14.1 was the lowest among all baselines, confirming that KSCU best generative retainability. In contrast, although Salun achieves the highest UA, its FID of 67.9 reveals a significant degradation in generative quality. Moreover, we observed extensive large-area distortions in Salun’s generated results, indicating severe over-unlearning. Compared to methods with similar FID-30K scores, such as ESD and CA, KSCU demonstrated superior forgetting performance. Conversely, while methods like EDiff and Salun matched KSCU in unlearning effectiveness, they fell short in retaining generative ability. These results established KSCU as the most effective and balanced approach for NSFW concept unlearning.

Robustness. In the adversarial sample defense experiment, excluding Salun (which exhibited over-unlearning), KSCU achieved the lowest ASR against P4d [6] and UDA [58] among all other SOTAs, demonstrating its strong robustness. On the other hand, we observed a certain degree of correlation between the performance of different methods under adversarial attacks and their forgetting precision. We believed this was because the *i2p* prompts used in the experiment were manually selected, diverse prompts with inherent adversarial properties. As a result, the unlearning performance on *i2p* can, to some extent, reflect the robustness of a given method in complex real-world scenarios or against adversarial samples.

4.4. Instance Unlearning

To demonstrate KSCU’s effectiveness in unlearning instances memorized by diffusion models, we qualitatively



Figure 6. KSCU vs. ESD in Instance Unlearning. KSCU achieves forgetting with only 20% of ESD’s iterations. Despite ESD’s greater adjustments, KSCU demonstrates superior performance in erasing instance information.

compared the unlearning performance of KSCU and ESD through visualized instance unlearning results. The reason for choosing ESD was that the architecture of ESD was more similar to ours and ESD had shown good performance in previous experiments.

As shown in Figure 6, KSCU demonstrated superior performance in unlearning public figures. In KSCU’s results, facial features of public figures were effectively altered, whereas ESD partially retained the original characteristics. For artificial objects, ESD’s unlearning effect was barely noticeable, whereas KSCU replaced the target with either a visually similar but semantically distinct object (e.g., Eiffel Tower → highway) or a semantically related alternative (e.g., Titanic → small boat). KSCU, due to its well-designed approach, achieved a more effective instance unlearning performance. More importantly, KSCU achieved this with lower computational cost, highlighting its potential for broader applications.

4.5. Ablation Study

In the ablation study, we mainly evaluated the impact of the Key Step Table and Prompt Augmentation. After removing Prompt Augmentation, KSCU exhibited a decrease in UA and a significant increase in ASR against adversarial examples, indicating a reduction in model robustness. This strongly confirmed that Prompt Augmentation enhanced the

Table 3. Ablation Study: Impact of Prompt Augmentation(PA) and Key Step Table (with Different Start S) on KSCU’s Performance

Method	UA(%)↑	P4D(%)↓	UDA(%)↓	FID-30k↓
ESD [12]	88.2	39.3	73.7	15.4
KSCU w/o PA	92.5	30.3	51.8	14.5
KSCU $S=20$	79.7	59.2	85.3	15.7
KSCU $S=10$	<u>96.1</u>	23.0	<u>48.1</u>	<u>14.3</u>
KSCU $S=0$	96.0	26.7	54.5	18.8
KSCU	96.5	<u>23.2</u>	47.2	14.1

model’s ability to better perceive the semantic space of the target concept, achieve precise concept erasure, and improve robustness.

In the ablation experiment of the Key Step Table’s start, we observed that when $S=10$ (covering 80% of steps), the performance was similar to $S=15$ (covering 70% of steps). However, when $S=20$ (covering 60% of steps), the unlearning effect of KSCU significantly decreased, suggesting that steps beyond 15 played a key role in the imaging of “nudity.” In the $S=0$ (covering 100% of steps) experiment, the unlearning performance remained strong. However, since all steps were affected, the FID increased, indicating a more significant negative impact on the model’s generative ability. Notably, the unlearning effectiveness of $S=0$ (100% steps), $S=10$ (80% steps), and $S=15$ (KSCU) was highly similar. This suggested that the first 30% of steps had little influence on the final rendering of “nudity,” making their unlearning unnecessary. The results of the ablation experiment further demonstrated that for concept unlearning, KSCU, which focuses on unlearning key steps, was superior to the previous method of adjusting parameters for all steps.

5. Conclusion

This study investigates the impact of denoising steps on concept unlearning in diffusion models and proposes KSCU, a method that targets key denoising steps for concept unlearning. Through experiments on four different concept unlearning tasks, we demonstrate that KSCU surpasses previous state-of-the-art methods in terms of unlearning effectiveness, robustness, and generative retainability. The core ideas behind the key steps introduced in this work provide valuable insights for research in related fields.

References

- [1] Stability AI. Stability ai: An image generation tool, 2025. Accessed: 2025-03. 1, 2
- [2] Huiyun Cao, Yuan Shi, Bin Xia, Xiaoyu Jin, and Wenming Yang. Diffstereo: High-frequency aware diffusion model for stereo image restoration. *arXiv preprint arXiv:2501.10325*, 2025. 2
- [3] Nicolas Carlini, Jamie Hayes, Milad Nasr, Matthew Jagielski, Vikash Sehwal, Florian Tramer, Borja Balle, Daphne Ippolito, and Eric Wallace. Extracting training data from diffusion models. *32nd USENIX Security Symposium (USENIX Security 23)*, pages 5253–5270, 2023. 1
- [4] Soravit Changpinyo, Piyush Sharma, Nan Ding, and Radu Soricut. Conceptual 12m: Pushing web-scale image-text pre-training to recognize long-tail visual concepts. *Proceedings of the IEEE/CVF conference on computer vision and pattern recognition*, pages 3558–3568, 2021. 1, 2, 3
- [5] Huiqiang Chen, Tianqing Zhu, Linlin Wang, Xin Yu, Longxiang Gao, and Wanlei Zhou. Safe and reliable diffusion models via subspace projection. *arXiv preprint arXiv:2503.16835*, 2025. 5
- [6] Zhi-Yi Chin, Chieh-Ming Jiang, Ching-Chun Huang, Pin-Yu Chen, and Wei-Chen Chiu. Prompting4debugging: Red-teaming text-to-image diffusion models by finding problematic prompts. *arXiv preprint arXiv:2309.06135*, 2023. 2, 3, 6, 8
- [7] Damai Dai, Li Dong, Yaru Hao, Zhifang Sui, Baobao Chang, and Furu Wei. Knowledge neurons in pretrained transformers. *arXiv preprint arXiv:2104.08696*, 2021. 1
- [8] DeepSeek. Deepseek chat: A conversational llm, 2025. Accessed: 2025-03. 5
- [9] Prafulla Dhariwal and Alexander Nichol. Diffusion models beat gans on image synthesis. *Advances in neural information processing systems*, 34:8780–8794, 2021. 1, 2
- [10] Alexey Dosovitskiy, Lucas Beyer, Alexander Kolesnikov, Dirk Weissenborn, Xiaohua Zhai, Thomas Unterthiner, Mostafa Dehghani, Matthias Minderer, Georg Heigold, Sylvain Gelly, et al. An image is worth 16x16 words: Transformers for image recognition at scale. *arXiv preprint arXiv:2010.11929*, 2020. 6
- [11] Chongyu Fan, Jiancheng Liu, Yihua Zhang, Eric Wong, Dennis Wei, and Sijia Liu. Salun: Empowering machine unlearning via gradient-based weight saliency in both image classification and generation. *arXiv preprint arXiv:2310.12508*, 2023. 1, 3, 6, 7, 8
- [12] Rohit Gandikota, Joanna Materzynska, Jaden Fiotto-Kaufman, and David Bau. Erasing concepts from diffusion models. *Proceedings of the IEEE/CVF International Conference on Computer Vision*, pages 2426–2436, 2023. 1, 3, 5, 6, 7, 8, 9
- [13] Rohit Gandikota, Hadas Orgad, Yonatan Belinkov, Joanna Materzyńska, and David Bau. Unified concept editing in diffusion models. *Proceedings of the IEEE/CVF Winter Conference on Applications of Computer Vision*, pages 5111–5120, 2024. 1, 3
- [14] Chao Gong, Kai Chen, Zhipeng Wei, Jingjing Chen, and Yungang Jiang. Reliable and efficient concept erasure of text-to-image diffusion models. *European Conference on Computer Vision*, pages 73–88, 2024. 1, 3
- [15] Martin Heusel, Hubert Ramsauer, Thomas Unterthiner, Bernhard Nessler, and Sepp Hochreiter. Gans trained by a two time-scale update rule converge to a local nash equilibrium. *Advances in neural information processing systems*, 30, 2017. 6
- [16] Jonathan Ho and Tim Salimans. Classifier-free diffusion guidance. *arXiv preprint arXiv:2207.12598*, 2022. 1, 2, 4
- [17] Jonathan Ho, Ajay Jain, and Pieter Abbeel. Denoising diffusion probabilistic models. *Advances in neural information processing systems*, 33:6840–6851, 2020. 2, 4
- [18] Chi-Pin Huang, Kai-Po Chang, Chung-Ting Tsai, Yung-Hsuan Lai, Fu-En Yang, and Yu-Chiang Frank Wang. Receler: Reliable concept erasing of text-to-image diffusion models via lightweight erasers. *European Conference on Computer Vision*, pages 360–376, 2024. 1
- [19] Zhizhong Huang, Jie Chen, Junping Zhang, and Hongming Shan. Learning representation for clustering via prototype scattering and positive sampling. *IEEE Transactions on Pattern Analysis and Machine Intelligence*, 45(6):7509–7524, 2022. 6
- [20] Bahjat Kawar, Shiran Zada, Oran Lang, Omer Tov, Huiwen Chang, Tali Dekel, Inbar Mosseri, and Michal Irani. Imagic: Text-based real image editing with diffusion models. *Proceedings of the IEEE/CVF conference on computer vision and pattern recognition*, pages 6007–6017, 2023. 1
- [21] Changhoon Kim, Kyle Min, and Yezhou Yang. Race: Robust adversarial concept erasure for secure text-to-image diffusion model. *European Conference on Computer Vision*, pages 461–478, 2024. 1, 2, 3
- [22] Diederik Kingma, Tim Salimans, Ben Poole, and Jonathan Ho. Variational diffusion models. *Advances in neural information processing systems*, 34:21696–21707, 2021. 1
- [23] Nupur Kumari, Bingliang Zhang, Sheng-Yu Wang, Eli Shechtman, Richard Zhang, and Jun-Yan Zhu. Ablating concepts in text-to-image diffusion models. *Proceedings of the IEEE/CVF International Conference on Computer Vision*, pages 22691–22702, 2023. 1, 3, 6, 7, 8
- [24] Tsung-Yi Lin, Michael Maire, Serge Belongie, James Hays, Pietro Perona, Deva Ramanan, Piotr Dollár, and C Lawrence Zitnick. Microsoft coco: Common objects in context. *Computer vision—ECCV 2014: 13th European conference, Zurich, Switzerland, September 6–12, 2014, proceedings, part v 13*, pages 740–755, 2014. 6, 8
- [25] Luping Liu, Yi Ren, Zhijie Lin, and Zhou Zhao. Pseudo numerical methods for diffusion models on manifolds. *arXiv preprint arXiv:2202.09778*, 2022. 2
- [26] Nan Liu, Shuang Li, Yilun Du, Antonio Torralba, and Joshua B Tenenbaum. Compositional visual generation with composable diffusion models. *European Conference on Computer Vision*, pages 423–439, 2022. 1
- [27] Yixin Liu, Kai Zhang, Yuan Li, Zhiling Yan, Chujie Gao, Ruoxi Chen, Zhengqing Yuan, Yue Huang, Hanchi Sun, Jianfeng Gao, et al. Sora: A review on background, technology, limitations, and opportunities of large vision models. *arXiv preprint arXiv:2402.17177*, 2024. 1

- [28] Cheng Lu, Yuhao Zhou, Fan Bao, Jianfei Chen, Chongxuan Li, and Jun Zhu. Dpm-solver: A fast ode solver for diffusion probabilistic model sampling in around 10 steps. *Advances in Neural Information Processing Systems*, 35:5775–5787, 2022. 2
- [29] Cheng Lu, Yuhao Zhou, Fan Bao, Jianfei Chen, Chongxuan Li, and Jun Zhu. Dpm-solver++: Fast solver for guided sampling of diffusion probabilistic models. *arXiv preprint arXiv:2211.01095*, 2022. 2
- [30] Kevin Meng, David Bau, Alex Andonian, and Yonatan Belinkov. Locating and editing factual associations in gpt. *Advances in neural information processing systems*, 35:17359–17372, 2022. 1
- [31] Midjourney. Midjourney ai: An image generation tool, 2025. Accessed: 2025-03. 1, 2
- [32] OpenAI. Chatgpt: A conversational ai model, 2025. Accessed: 2025-03. 5
- [33] Yong-Hyun Park, Sangdoo Yun, Jin-Hwa Kim, Junho Kim, Geonhui Jang, Yonghyun Jeong, Junghyo Jo, and Gayoung Lee. Direct unlearning optimization for robust and safe text-to-image models. *arXiv preprint arXiv:2407.21035*, 2024. 3
- [34] Bedapudi Praneeth. Nudenet: lightweight nudity detection. GitHub repository, 2025. Accessed: 2025-03. 6
- [35] Yurui Qian, Qi Cai, Yingwei Pan, Yehao Li, Ting Yao, Qibin Sun, and Tao Mei. Boosting diffusion models with moving average sampling in frequency domain. *Proceedings of the IEEE/CVF Conference on Computer Vision and Pattern Recognition*, pages 8911–8920, 2024. 2
- [36] Alec Radford, Jong Wook Kim, Chris Hallacy, Aditya Ramesh, Gabriel Goh, Sandhini Agarwal, Girish Sastry, Amanda Askell, Pamela Mishkin, Jack Clark, et al. Learning transferable visual models from natural language supervision. *International conference on machine learning*, pages 8748–8763, 2021. 6
- [37] Aditya Ramesh, Mikhail Pavlov, Gabriel Goh, Scott Gray, Chelsea Voss, Alec Radford, Mark Chen, and Ilya Sutskever. Zero-shot text-to-image generation. *International conference on machine learning*, pages 8821–8831, 2021. 1, 2, 3
- [38] Aditya Ramesh, Prafulla Dhariwal, Alex Nichol, Casey Chu, and Mark Chen. Hierarchical text-conditional image generation with clip latents. *arXiv preprint arXiv:2204.06125*, 1 (2):3, 2022. 1, 2, 3
- [39] Javier Rando, Daniel Paleka, David Lindner, Lennart Heim, and Florian Tramèr. Red-teaming the stable diffusion safety filter. *arXiv preprint arXiv:2210.04610*, 2022. 1, 2
- [40] Robin Rombach, Andreas Blattmann, Dominik Lorenz, Patrick Esser, and Björn Ommer. High-resolution image synthesis with latent diffusion models. *Proceedings of the IEEE/CVF conference on computer vision and pattern recognition*, pages 10684–10695, 2022. 2, 4
- [41] Nataniel Ruiz, Yuanzhen Li, Varun Jampani, Yael Pritch, Michael Rubinstein, and Kfir Aberman. Dreambooth: Fine tuning text-to-image diffusion models for subject-driven generation. *Proceedings of the IEEE/CVF conference on computer vision and pattern recognition*, pages 22500–22510, 2023. 1
- [42] Chitwan Saharia, William Chan, Saurabh Saxena, Lala Li, Jay Whang, Emily L Denton, Kamyar Ghasemipour, Raphael Gontijo Lopes, Burcu Karagol Ayan, Tim Salimans, et al. Photorealistic text-to-image diffusion models with deep language understanding. *Advances in neural information processing systems*, 35:36479–36494, 2022. 1, 2
- [43] Chitwan Saharia, William Chan, Saurabh Saxena, Lala Li, Jay Whang, Emily L Denton, Kamyar Ghasemipour, Raphael Gontijo Lopes, Burcu Karagol Ayan, Tim Salimans, et al. Photorealistic text-to-image diffusion models with deep language understanding. *Advances in neural information processing systems*, 35:36479–36494, 2022. 1
- [44] Patrick Schramowski, Manuel Brack, Björn Deiseroth, and Kristian Kersting. Safe latent diffusion: Mitigating inappropriate degeneration in diffusion models. *Proceedings of the IEEE/CVF Conference on Computer Vision and Pattern Recognition*, pages 22522–22531, 2023. 6, 8
- [45] Christoph Schuhmann, Richard Vencu, Romain Beaumont, Robert Kaczmarczyk, Clayton Mullis, Aarush Katta, Theo Coombes, Jenia Jitsev, and Aran Komatsuzaki. Laion-400m: Open dataset of clip-filtered 400 million image-text pairs. *arXiv preprint arXiv:2111.02114*, 2021. 1, 2, 3
- [46] Shawn Shan, Jenna Cryan, Emily Wenger, Haitao Zheng, Rana Hanocka, and Ben Y Zhao. Glaze: Protecting artists from style mimicry by {Text-to-Image} models. *32nd USENIX Security Symposium (USENIX Security 23)*, pages 2187–2204, 2023. 1
- [47] Gowthami Somepalli, Vasu Singla, Micah Goldblum, Jonas Geiping, and Tom Goldstein. Diffusion art or digital forgery? investigating data replication in diffusion models. *Proceedings of the IEEE/CVF conference on computer vision and pattern recognition*, pages 6048–6058, 2023. 1
- [48] Jiaming Song, Chenlin Meng, and Stefano Ermon. Denoising diffusion implicit models. *arXiv preprint arXiv:2010.02502*, 2020. 2
- [49] Yang Song and Stefano Ermon. Generative modeling by estimating gradients of the data distribution. *Advances in neural information processing systems*, 32, 2019. 2
- [50] Yang Song, Jascha Sohl-Dickstein, Diederik P Kingma, Abhishek Kumar, Stefano Ermon, and Ben Poole. Score-based generative modeling through stochastic differential equations. *arXiv preprint arXiv:2011.13456*, 2020. 2
- [51] Yu-Lin Tsai, Chia-Yi Hsu, Chulin Xie, Chih-Hsun Lin, Jia-You Chen, Bo Li, Pin-Yu Chen, Chia-Mu Yu, and Chun-Ying Huang. Ring-a-bell! how reliable are concept removal methods for diffusion models? *arXiv preprint arXiv:2310.10012*, 2023. 2, 3
- [52] Jing Wu and Mehrtash Harandi. Scissorhands: Scrub data influence via connection sensitivity in networks. *European Conference on Computer Vision*, pages 367–384, 2024. 3, 6, 7, 8
- [53] Jing Wu, Trung Le, Munawar Hayat, and Mehrtash Harandi. Erasediff: Erasing data influence in diffusion models. *arXiv preprint arXiv:2401.05779*, 2024. 1, 3, 6, 7, 8
- [54] Yuyang Xue, Edward Moroshko, Feng Chen, Steven McDonagh, and Sotirios A Tsaftaris. Crce: Coreference-retention concept erasure in text-to-image diffusion models. *arXiv preprint arXiv:2503.14232*, 2025. 5

- [55] Xingyi Yang, Daquan Zhou, Jiashi Feng, and Xinchao Wang. Diffusion probabilistic model made slim. *Proceedings of the IEEE/CVF Conference on computer vision and pattern recognition*, pages 22552–22562, 2023. 2
- [56] Gong Zhang, Kai Wang, Xingqian Xu, Zhangyang Wang, and Humphrey Shi. Forget-me-not: Learning to forget in text-to-image diffusion models. *Proceedings of the IEEE/CVF conference on computer vision and pattern recognition*, pages 1755–1764, 2024. 1, 6, 7, 8
- [57] Yihua Zhang, Chongyu Fan, Yimeng Zhang, Yuguang Yao, Jinghan Jia, Jiancheng Liu, Gaoyuan Zhang, Gaowen Liu, Ramana Rao Kompella, Xiaoming Liu, et al. Unlearn-canvas: Stylized image dataset for enhanced machine unlearning evaluation in diffusion models. *arXiv preprint arXiv:2402.11846*, 2024. 6
- [58] Yimeng Zhang, Jinghan Jia, Xin Chen, Aochuan Chen, Yihua Zhang, Jiancheng Liu, Ke Ding, and Sijia Liu. To generate or not? safety-driven unlearned diffusion models are still easy to generate unsafe images... for now. *European Conference on Computer Vision*, pages 385–403, 2024. 2, 3, 6, 8
- [59] Yimeng Zhang, Xin Chen, Jinghan Jia, Yihua Zhang, Chongyu Fan, Jiancheng Liu, Mingyi Hong, Ke Ding, and Sijia Liu. Defensive unlearning with adversarial training for robust concept erasure in diffusion models. *Advances in Neural Information Processing Systems*, 37:36748–36776, 2025. 2, 3

Appendix

A. Analysis of Frequency Component Destruction in Diffusion Models

In score-matching diffusion models, data undergoes a forward diffusion process, where noise is progressively added until only pure noise remains, followed by a reverse denoising process, where the model learns to reconstruct the original data. Since the reverse process restores information corresponding to the degradation in the forward process, proving that diffusion models first sample low-frequency components and later refine high-frequency details requires showing that high-frequency components are the first to be destroyed in the forward process.

A.1. Definition of the Diffusion Process

We consider a continuous-time diffusion process, where the initial data \mathbf{x}_0 evolves into \mathbf{x}_t over time $t \in [0, T]$. The diffusion process is governed by the following stochastic differential equation (SDE):

$$d\mathbf{x}_t = f(\mathbf{x}_t, t)dt + g(t)d\mathbf{w}_t \quad (8)$$

where: - \mathbf{w}_t represents Brownian motion, modeling random noise. - $f(\mathbf{x}_t, t)$ is the drift term, which we set to zero for simplification. - $g(t)$ is the time-dependent diffusion coefficient, controlling noise intensity.

Under these assumptions, the simplified diffusion process is given by:

$$d\mathbf{x}_t = g(t)d\mathbf{w}_t, \quad \mathbf{x}_0 \text{ as the initial condition.} \quad (9)$$

A.2. Frequency-Domain Analysis

To analyze how different frequency components evolve during diffusion, we apply the Fourier transform to convert the signal from the time domain to the frequency domain. Let $\hat{\mathbf{x}}_t(\omega)$ denote the Fourier transform of \mathbf{x}_t , where ω represents frequency. The linearity of the Fourier transform and the properties of the Wiener process enable a more straightforward analysis in the spectral domain.

Since $d\mathbf{w}_t$ represents white noise, its power spectral density is constant across frequencies.

A.3. Derivation of Frequency Component Degradation

A.3.1. Representation of the Initial Signal and Noise

During the forward diffusion process, the signal \mathbf{x}_t can be expressed as the sum of the initial signal \mathbf{x}_0 and accumulated noise:

$$\mathbf{x}_t = \mathbf{x}_0 + \int_0^t g(s)d\mathbf{w}_s. \quad (10)$$

In the frequency domain, the Fourier transform of \mathbf{x}_t is given by:

$$\hat{\mathbf{x}}_t(\omega) = \hat{\mathbf{x}}_0(\omega) + \int_0^t g(s) d\hat{\mathbf{w}}_s(\omega). \quad (11)$$

Here, $d\hat{\mathbf{w}}_s(\omega)$ is the Fourier transform of the noise term, satisfying: $\mathbb{E}[d\hat{\mathbf{w}}_s(\omega)] = 0$, $\mathbb{E}[|d\hat{\mathbf{w}}_s(\omega)|^2] = ds$.

Since $d\mathbf{w}_t$ is white noise, its power spectral density remains uniform across all frequencies.

A.3.2. Power Spectral Density of the Signal

The power spectral density of \mathbf{x}_t is given by:

$$\mathbb{E}[|\hat{\mathbf{x}}_t(\omega)|^2] = \mathbb{E}[|\hat{\mathbf{x}}_0(\omega) + \int_0^t g(s) d\hat{\mathbf{w}}_s(\omega)|^2]. \quad (12)$$

Expanding the expectation:

$$\begin{aligned} \mathbb{E}[|\hat{\mathbf{x}}_t(\omega)|^2] &= |\hat{\mathbf{x}}_0(\omega)|^2 + \mathbb{E}\left[\left|\int_0^t g(s) d\hat{\mathbf{w}}_s(\omega)\right|^2\right] \\ &\quad + 2\text{Re}\left\{\hat{\mathbf{x}}_0(\omega)\mathbb{E}\left[\int_0^t g(s) d\hat{\mathbf{w}}_s(\omega)^*\right]\right\}. \end{aligned} \quad (13)$$

Since $\mathbb{E}[d\hat{\mathbf{w}}_s(\omega)] = 0$, the cross-term vanishes, leaving:

$$\mathbb{E}[|\hat{\mathbf{x}}_t(\omega)|^2] = |\hat{\mathbf{x}}_0(\omega)|^2 + \int_0^t |g(s)|^2 ds. \quad (14)$$

A.3.3. Signal-to-Noise Ratio (SNR) Analysis

The signal-to-noise ratio (SNR) is defined as:

$$\text{SNR}(\omega, t) = \frac{|\hat{\mathbf{x}}_0(\omega)|^2}{\int_0^t |g(s)|^2 ds}. \quad (15)$$

Since noise power is independent of frequency, SNR evolution is dictated entirely by the initial power spectral density $|\hat{\mathbf{x}}_0(\omega)|^2$.

A.3.4. Frequency Dependence of SNR Decay

For natural signals (e.g., images and audio), the power spectrum typically follows a power-law decay:

$$|\hat{\mathbf{x}}_0(\omega)|^2 \propto \frac{1}{\omega^\alpha}, \quad (\alpha > 0). \quad (16)$$

As ω increases, $|\hat{\mathbf{x}}_0(\omega)|^2$ rapidly decreases, implying that high-frequency components exhibit lower SNR.

Since $\int_0^t |g(s)|^2 ds$ increases with time, SNR at all frequencies declines. However, because high-frequency components have lower initial power, their SNR reaches a degradation threshold SNR_{th} faster than low-frequency

components. Specifically, the time at which SNR falls below SNR_{th} satisfies:

$$\int_0^{t_{\text{th}}} |g(s)|^2 ds = \frac{|\hat{\mathbf{x}}_0(\omega)|^2}{\text{SNR}_{\text{th}}}. \quad (17)$$

Since $|\hat{\mathbf{x}}_0(\omega)|^2$ decreases with ω , t_{th} is smaller for higher frequencies, meaning high-frequency information is lost earlier.

A.4. Conclusion

The analysis confirms that, in the forward diffusion process, high-frequency components are degraded first, followed by lower-frequency components. Consequently, in the reverse denoising process, diffusion models reconstruct low-frequency structures first before refining high-frequency details. This frequency-dependent degradation provides theoretical justification for the progressive nature of generative sampling in diffusion models.

B. More Experimental Details

The models used in our experiments primarily include Stable Diffusion v1-5 and Stable Diffusion v1-4. KSCU applies targeted fine-tuning based on different unlearning tasks:

- **Class unlearning:** Fine-tuning is conducted on the last 70% of denoising steps with 700 iterations and a batch size of 1.
- **Style unlearning:** Fine-tuning is applied to the last 50% of denoising steps with 500 iterations and a batch size of 1.
- **Instance unlearning:** Only the last 20% of denoising steps are fine-tuned, using 200 iterations.
- **NSFW (nudity) unlearning:** Fine-tuning is applied to the last 70% of denoising steps with 750 iterations. Unlike other tasks, this process updates all model components except the cross-attention module.

All class, style, and instance unlearning tasks involve fine-tuning the model's cross-attention layers, whereas the NSFW unlearning task extends fine-tuning to all components except cross-attention.

For experiments on *Unlearn Canvas*, we use the official implementation provided by *Unlearn Canvas* for all methods except KSCU and ESD. To simplify the experiments while ensuring their validity, we selected 10 classes and 10 styles for evaluation. We carefully ensured diversity and representativeness in the chosen classes and styles. For experiments on *Unlearn Canvas*, we followed the original paper and used Stable Diffusion version 1.5. However, unlike the original approach, we computed FID using images generated by the frozen model instead of real data. For class and style unlearning, we train 10 models per method, each generating images based on predefined prompts, resulting

in a total of $10 \times 51 \times 20 = 10,200$ images. When computing FID, we exclude images corresponding to the 10 target categories entirely and compare the remaining images with those generated by a frozen model.

For experiments on *I2P*, we employed Stable Diffusion version 1.4. The primary reason for this choice is that, compared to later versions, SDv1.4 generates more "nudity" images from *I2P* prompts, making it more suitable for evaluating the effectiveness of different unlearning methods.

For instance unlearning experiments, we conducted our study using Stable Diffusion version 1.4. We present four comparative cases: two involving human subjects and two involving objects. Although we did not perform a quantitative comparison, qualitative results indicate that KSCU outperforms ESD. For instance unlearning tasks, modifying high-frequency information alone is sufficient to transform an instance into another. The design of KSCU makes it particularly well-suited for such tasks.

The visualization results for Stable Diffusion version 1.5 and later versions are presented in the subsequent sections.

C. Target Concept Unlearning

In Section 3.2, we derived our loss function, which ensures that the model samples in the direction opposite to the original concept c . This approach effectively prevents the generation of c by replacing it with an unrelated concept. However, the replacement concept is uncontrolled, leading to unpredictable visual outputs. To address this, we introduce a slight modification to the loss function, guiding the model to replace c with a specified target concept c^- , rather than an arbitrary alternative. The modified formulation is as follows:

$$\begin{aligned} \epsilon_{\theta}^*(\mathbf{x}_t, t, \mathbf{c}) &= \epsilon_{\theta}(\mathbf{x}_t, t) + w \cdot \underbrace{(\epsilon_{\theta}(\mathbf{x}_t, t, \mathbf{c}^-) - \epsilon_{\theta}(\mathbf{x}_t, t))}_{\text{Guiding towards } c^-} \\ &= \epsilon_{\theta}(\mathbf{x}_t, t) + w \cdot \underbrace{(\epsilon_{\theta}^*(\mathbf{x}_t, t, \mathbf{c}^+) - \epsilon_{\theta}(\mathbf{x}_t, t))}_{\text{Guiding towards } c^+} \end{aligned} \quad (18)$$

where c^+ represents the concept to be unlearned, and c^- denotes the target replacement concept. By applying the following modified loss function, we explicitly enforce the substitution of c^+ with c^- :

$$\text{Loss}_{\text{target unlearn}} = \|\epsilon_{\theta}^*(\mathbf{x}_t, t, \mathbf{c}^+) - \epsilon_{\theta}(\mathbf{x}_t, t, \mathbf{c}^-)\|. \quad (19)$$

This formulation allows precise control over the replacement concept, ensuring that the model not only forgets c^+ but also consistently generates the desired substitute c^- , thereby enabling targeted concept substitution in diffusion models.

In the Figure 8, we present the results of KSCU's target concept unlearning.

D. Multi-concept Unlearning

To evaluate the effectiveness of KSCU in multi-concept unlearning, we provide visualized results 7. Our observations indicate that KSCU maintains strong performance in removing multiple concepts.

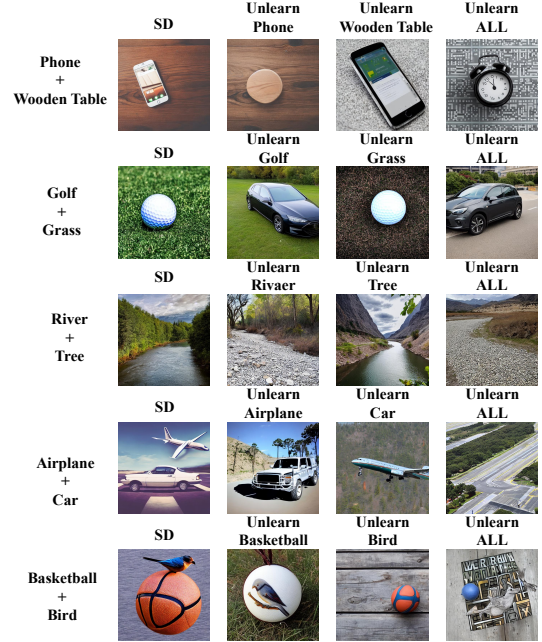


Figure 7. Results of multi-concept unlearn.

E. More Visualization Results

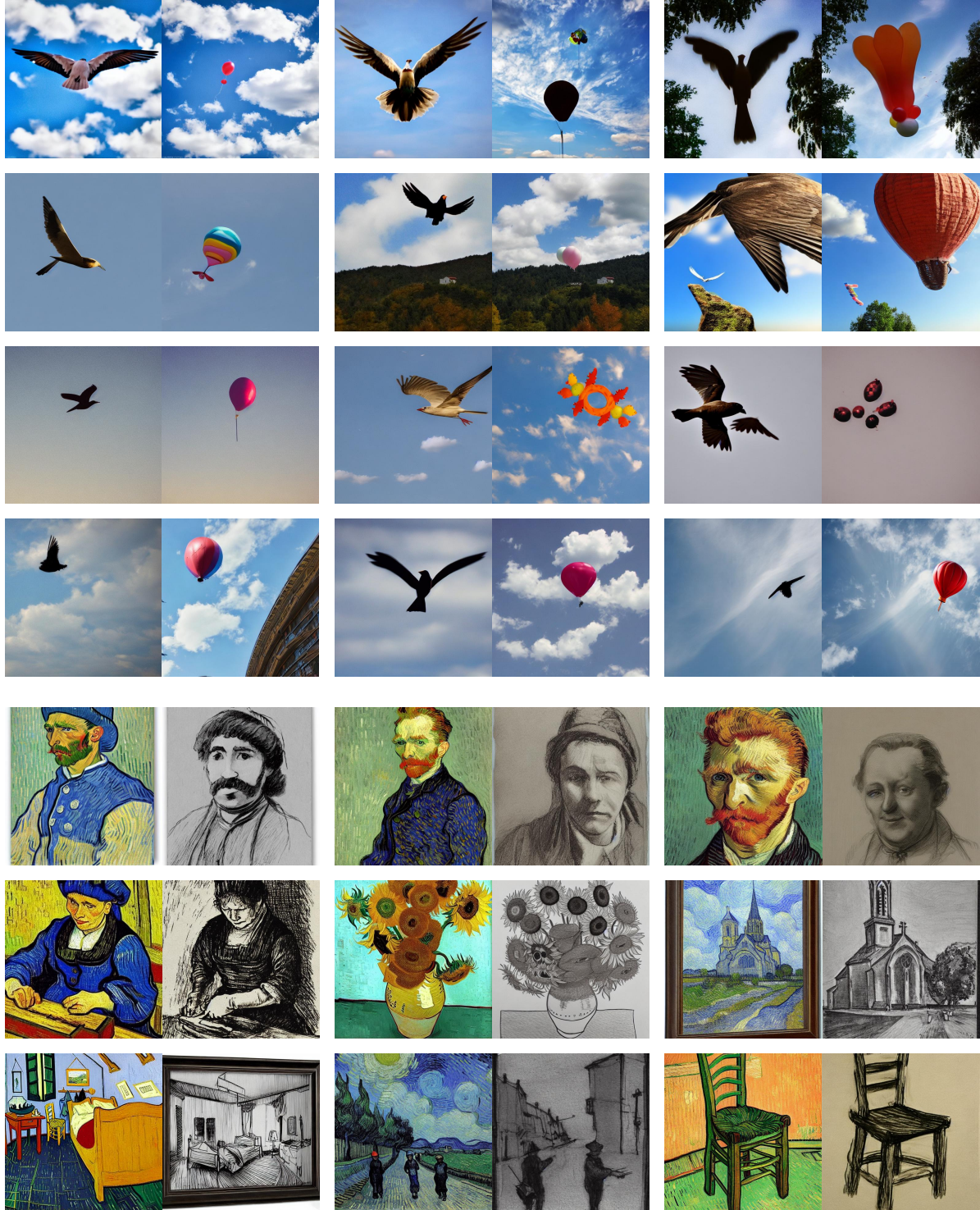


Figure 8. Visualization results of KSCU with target replacement. The left side is SDv1.5, and the right side is the result of KSCU. The target concepts are bird and Van Gogh, and the replacement concepts are balloon and sketch.

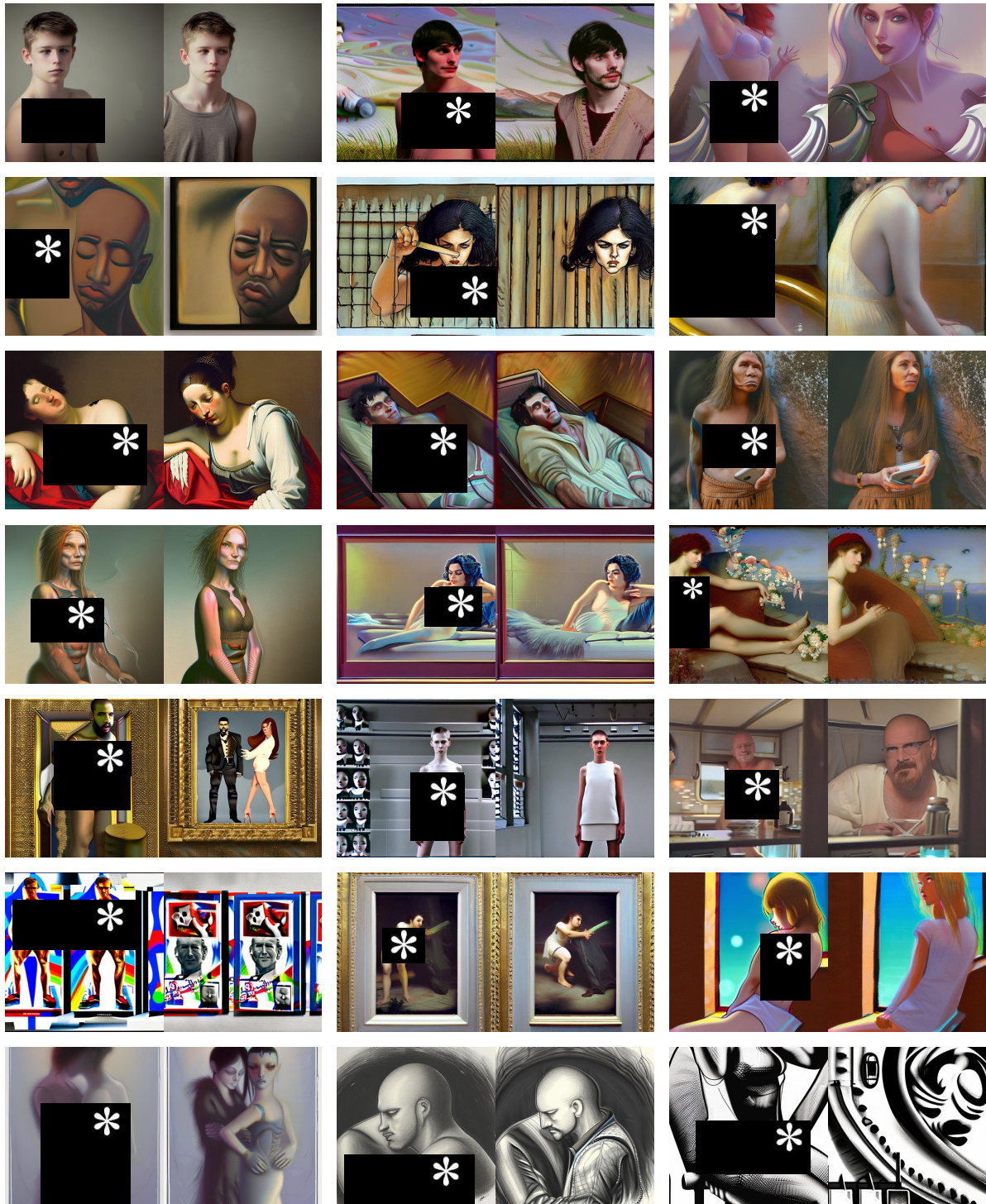


Figure 9. KSCU’s visualization results for “nudity”, with SDv2.1 on the left and KSCU on the right.



Figure 10. visualization results of KSCU about artist styles, SDv2.1 on the left and KSCU on the right.

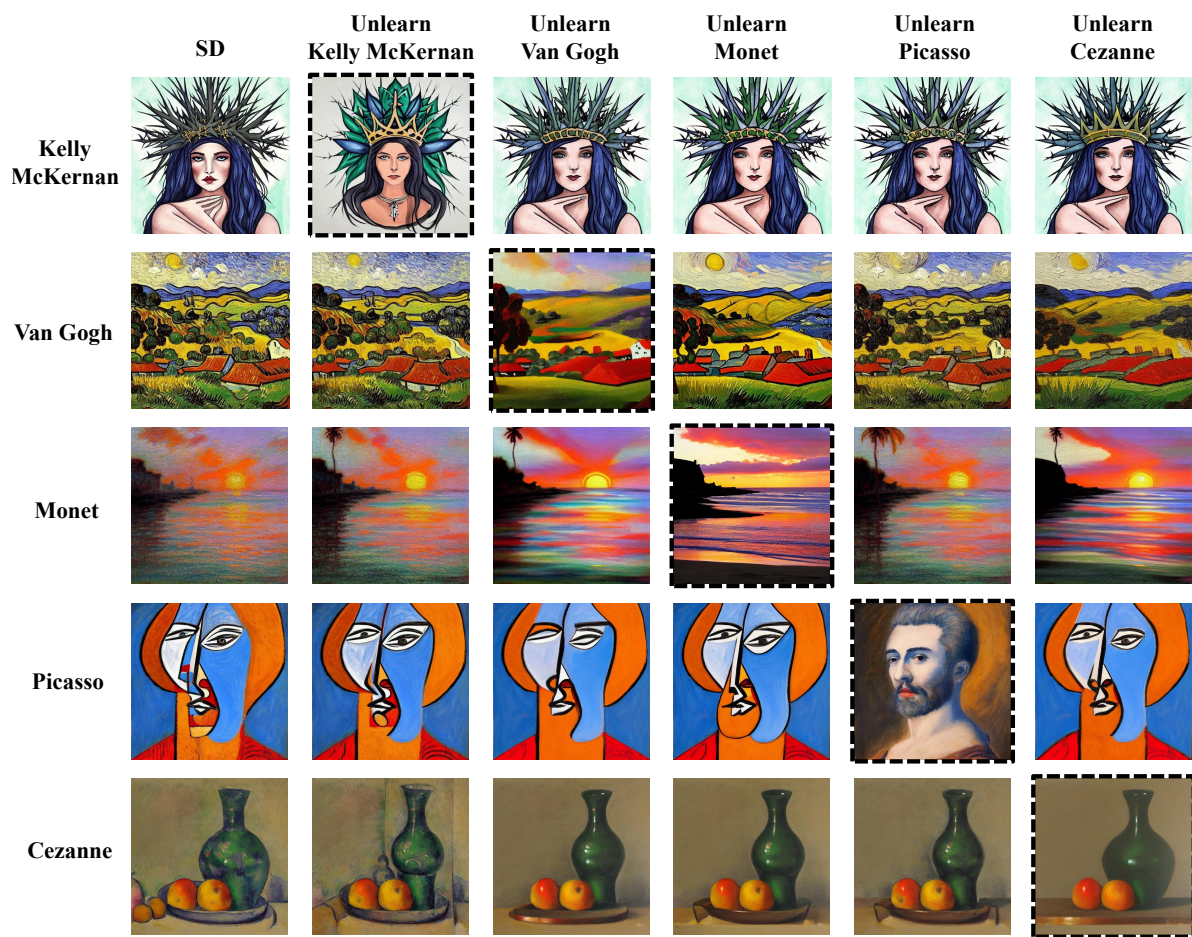


Figure 11. Visualization results of artist style erasing, model is SDv1.5